AIP | Applied Physics Letters

Ultra broadband phase measurements on nanostructured metasurfaces

E. Pshenay-Severin, M. Falkner, C. Helgert, and T. Pertsch

Citation: Applied Physics Letters **104**, 221906 (2014); doi: 10.1063/1.4881332
View online: http://dx.doi.org/10.1063/1.4881332
View Table of Contents: http://scitation.aip.org/content/aip/journal/apl/104/22?ver=pdfcov
Published by the AIP Publishing

Ultra broadband phase measurements on nanostructured metasurfaces

E. Pshenay-Severin,[1,2,a)] M. Falkner,[1] C. Helgert,[1] and T. Pertsch[1]
[1]*Institute of Applied Physics, Abbe Center of Photonics, Friedrich-Schiller-Universität Jena, Max-Wien-Platz 1, 07743 Jena, Germany*
[2]*Nonlinear Physics Center, Research School of Physics and Engineering, Australian National University, Mills Road 59, ACT 0200 Canberra, Australia*

(Received 15 November 2013; accepted 22 May 2014; published online 4 June 2014)

We report on an interferometric method developed for ultra broadband (from $\lambda = 0.65\,\mu$m to $\lambda = 1.7\,\mu$m) phase measurements on metasurfaces in transmission and reflection. Due to a unique performance of our method in terms of the accessible spectral range, accuracy (± 0.02 rad), and flexibility with respect to the sample arrangement, this technique can be broadly used as a versatile tool for the comprehensive characterization of a broad class of dispersive optical materials. We compare our experimental technique with an indirect approach and based on the Kramers-Kronig transformation analysis, establish a rule for the use of the indirect method. © *2014 AIP Publishing LLC*. [http://dx.doi.org/10.1063/1.4881332]

The design and creation of two-dimensional nanostructured materials have created a paradigm in material science: so-called metasurfaces have emerged as a class of integrated photonic elements featuring only a single or few surface layers composed of subwavelength plasmonic nanostructures.[1] Recently, significant breakthroughs in the wave front manipulation, such as abnormal and out-of-plane refraction and reflection, have been achieved by laterally inhomogeneous metasurfaces.[2,3] Another example is the spectrally selective image formation demonstrated by computationally encoded metasurfaces using the principles of digital holography.[4,5] In the view of the growing structural complexity of contemporary metasurfaces, the lack of comprehensive experimental methods to assess and characterize their building blocks performance becomes a critical issue, hampering development of this field towards real-world applications. Due to restrictions of the state-of-the-art experimental techniques for the phase measurements on metasurfaces, the preference is commonly given to indirect characterization methods relying heavily on rigorous numerical simulations.[6–12] Here, we demonstrate, based on the Kramers-Kronig transformation analysis, that the use of indirect methods is inadequate for the accurate characterization of complex metasurfaces. In order to provide experimental access to the complex transmission and reflection coefficients of optical metasurfaces and as a prerequisite to assess their broadband performance, we developed an original experimental technique. This technique enables to measure the absolute phase both in transmission and reflection in an ultra broadband spectral range. This extreme bandwidth together with the lacking necessity of additional physical assumptions, structuring of the samples, or demanding gauging procedures are the key features distinguishing the approach from previously proposed methods for phase measurements on metamaterials and metasurfaces.[6–12]

Shaping light propagation in optically passive media commonly requires the information on the light dispersion in a material, an issue that in the case of metasurfaces can be reduced to the problem of finding complex transmission and reflection coefficients $t(\lambda)$ and $r(\lambda)$. A main feature of metasurfaces is their capability of strong and resonant light interaction with the constitutive plasmonic nanostructures. Hence, the intensity, the phase, and the polarization state of light can be manipulated in extensive ranges with metasurfaces having thicknesses of only dozens of nanometers. Since simultaneous measurement of complex transmission and reflection on ultra-thin metasurfaces is still a challenging experimental issue, a method based on the combination of experimental data and numerical simulations is commonly applied. This indirect method requires measurements of the transmittance $T(\lambda)$ and reflectance $R(\lambda)$ using standard spectroscopic technique. With $T(\lambda)$ and $R(\lambda)$ being the squared moduli of the complex entities $t(\lambda)$ and $r(\lambda)$, no phase information is conveyed. Contrariwise, phase information is rather estimated from additional numerical simulations supposing a sufficient correspondence of simulated and measured $T(\lambda)$ and $R(\lambda)$. Though the indirect approach is broadly used, no clear rule for its use has been established until now. Here, we derive a general guideline using the Kramers-Kronig transformation method.[13]

Let us consider first the case of transmission trough a metasurface. For a complex transmission coefficient $t(\omega) = |t(\omega)|\exp[i\phi_t(\omega)]$, one can write: $\ln t(\omega) = \ln|t(\omega)| + i\phi_t(\omega)$. According to the Kramers-Kronig relation for the real and imaginary parts of a finite, analytical complex function, $\ln t(\omega)$, the phase is

$$\phi_t(\omega) = \frac{-2\omega}{\pi} P \int_0^\infty \frac{\ln|t(\omega')|}{\omega'^2 - \omega^2} d\omega', \tag{1}$$

where P signifies the principal value of the integral and $\omega = 2\pi c/\lambda$.[14] The relation (1) expresses the dependency of the phase of the transmission coefficient at a certain frequency on its amplitude in the whole spectral range. The same relation as for the complex transmission coefficient holds for the normalized reflection coefficient, which is commonly introduced instead of the reflection coefficient

a)Author to whom correspondence should be addressed. Electronic mail: katja.severin@uni-jena.de.

$r(\omega) = |r(\omega)|\exp[i\phi_r(\omega)]$ in order to satisfy the condition $r_{norm}(\omega) \to 1$ at $\omega \to \infty$.[13]

In general, the quantitative implementation of the Kramers-Kronig transformation to $\ln t(\omega)$ and $\ln r_{norm}(\omega)$ requires the introduction of a consistent physical model which adequately describes a system's spectral behavior within a spectral range of interest and provides an analytical form for $t(\omega)$ and $r(\omega)$ beyond this range. In the case of metasurfaces, this range of interest lies in the spectral region where the plasmonic resonances of their constitutive nanostructures dominate the optical response. Commonly, the experimental characterization of metasurfaces is also narrowed to this spectral region. Thus, the contributions to the phase of the amplitudes from the experimentally inaccessible spectral regions can be calculated using an analytical material model under assumption of monotonic behavior of the complex coefficients outside the spectral region of interest. It is worth noting that in plasmonic structures at resonance frequencies, the case of zero transmission or reflection can occur causing poles of the logarithmic functions. This mathematical issue can be treated in analogy to stratified media, where zero transmission occurs due to interference.[15] Nevertheless, the dependency of the phase at a certain wavelength on the amplitude of the respective spectral coefficient holds for metasurfaces in a general sense. Thus, only a good agreement of simulated and measured transmittance and reflectance in a broad spectral region, where plasmonic resonances of a structure dominate its spectral behavior, allows for using phase information from the numerical simulations. Commonly, though, this condition is not taken into consideration, and the local fitting of the amplitudes is considered as satisfied in order to define the phase information from numerical simulations. In particular cases, the discrepancies due to a not perfectly matched modeling of the geometrical parameters of real-world nanostructures can be resolved by rather involved numerical efforts, which are, however, unpractical to be implemented for every individual metasurface.[16] Thus, comprehensive experimental characterization of light dispersion on metasurfaces is the only trustful way to access their optical properties. In order to provide an ultra broadband phase measurement technique, we developed our original approach exploiting the principles of white light Fourier-transform spectral interferometry.[17] This technique requires the realization of a time delay τ between two beams of an interferometer using different geometrical lengths of its two arms. Under illumination with white light, this results in the formation of an interference pattern in the frequency domain. Our interferometric setup presented in Fig. 1 is a polarization interferometer modified for simultaneous measurements in transmission and reflection. The two arms of the interferometer are formed in the calcite beam displacer B1, where linear polarized light is split into two orthogonally polarized beams. The second displacer B2 serves to recombine the two beams and is followed by a linear polarizer P2, providing interference of the sample and reference beams. The recombined beam is coupled into a photonic crystal single mode fiber and delivered to an optical spectrum analyzer (OSA) providing spectral resolution up to 20 pm in the spectral range from $\lambda = 0.6\,\mu$m to $\lambda = 1.7\,\mu$m. Measurements of the phase in reflection are realized with the beam splitter, BS. The length difference between two arms of about 1 mm is achieved using compensating plates D1 and D2 made of BK7 with thicknesses 6 mm. The measured quantity is an interference signal of the two waves originating from the two interferometer arms in the wavelength domain. The retrieval of the phase delay between two arms requires to transform the measured data into the frequency domain, to Fourier transform this interferogram into the time domain, to filter an interference term, to back-Fourier transform the filtered term into the wavelength domain, and to finally take its argument. A detailed description of the mathematical apparatus of white-light interferometry can be found elsewhere.[17–19] The retrieved phase $\Delta\phi^s(\lambda) = \phi_{sam}(\lambda) - \phi_{ref}(\lambda)$ is the difference phase delay between the signals passing the sample arm $\phi_{sam}(\lambda)$ and the reference arm $\phi_{ref}(\lambda)$ of the interferometer. A reference measurement using an object with known optical properties is required for the extraction of the absolute phase due to the sample. As state-of-the-art metasurfaces have typical thicknesses smaller than 100 nm, any misalignment of the sample on the nanometer scale between the sample and reference measurements will cause a critical error in the resulting absolute phase.[18,20] We have solved this challenge by enabling simultaneous reference measurements without moving the sample. In order to apply this technique, the only requirement is the presence of a reference area with known optical properties in the close vicinity to the metasurface area. In our experiments, the samples contain an uncovered substrate adjacent to the metasurface area to be used as a reference object (see Fig. 1(b)). During the measurements, the sample is adjusted as shown in Figs. 1(c) and 1(d). The sample measurements are realized using the aperture A placed before the sample and arranged to screen one half of the two beams, as it is shown in Fig. 1(c). The position of the movable aperture is controlled with a camera collecting the light reflected from the filter placed after the sample (not shown in Fig. 1). During the reference measurements, the aperture blocks the other half of the beams as shown in Fig. 1(d). Performing the reference measurements using the pure substrate in transmission and reflection gives the phase difference $\Delta\phi^r = \phi_{sam}^{substrate}(\lambda) - \phi_{ref}(\lambda)$. Thus, taking into account the accumulated phase delay due to the dispersive optical elements and the geometrical length difference between the two arms, the phase delay accumulated by light propagating through a metasurface can be extracted from sample and reference measurements. In the general case, the retrieved phase bears an ambiguity of 2π, for metasurfaces, though, the measured phase in transmission can be safely assumed to be $-\pi < \phi_{msurf} < \pi$ at the wavelength of interest. The accuracy of the method is determined by the signal to noise ratio of the interference signal acquisition, which depends on the transmission (reflection) properties of a metasurface and is better than 0.02 rad for transmittance (reflectance) of at least 5%.

In our implementation, the moveable aperture A brings the drawback of undesired diffraction of the light beams and introduces an additional phase delay between the sample and reference measurements. To account for this delay, a normalization procedure had to be performed once before starting the sample characterization. For this purpose, two measurements without any sample are performed with the aperture

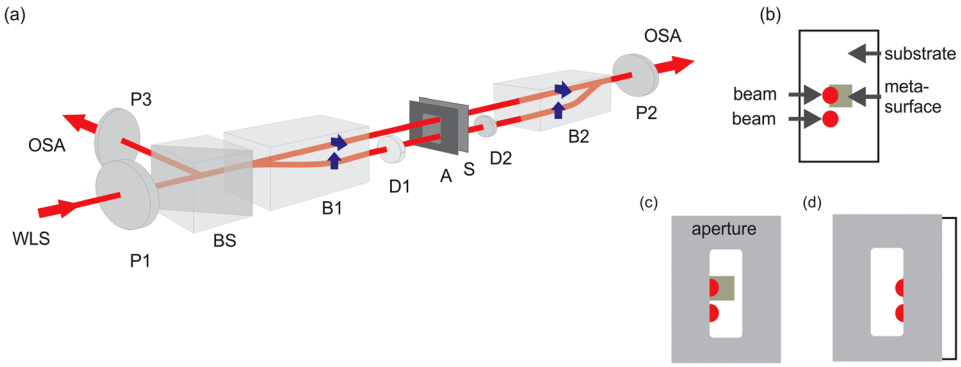

FIG. 1. (a) Interferometric setup. P1, P2, P3—Polarizers. BS—Beamsplitter. B1, B2—Beam displacers. D1, D2—Delay elements. A—Aperture. S—sample. (b) Sample layout. (c) and (d) Position of the aperture during sample and reference measurements.

blocking the left and the right halves of the beams, respectively. In the absence of a sample, the two measured phases ($\phi_1(\lambda)$ and $\phi_2(\lambda)$) have to be equal. However, due to the diffraction of the beams on the aperture, the measured phases are different $\phi_1(\lambda) \neq \phi_2(\lambda)$. Subtraction of the phases obtained from the two measurements gives the normalization value $\phi_n(\lambda) = \phi_1(\lambda) - \phi_2(\lambda)$, which is later subtracted from the phases measured on the samples.

Now, we will compare results for the phase definition using direct and indirect methods on two metasurfaces. The first metasurface we consider here consists of the gold nanodiscs shown in Fig. 2(a). Based on scanning micrograph images, an optimized model accounting for the true shape of the discs is implemented in the numerical simulations which were based on the Fourier modal method.[21] The simulated and measured spectra and phases are presented in Figs. 2(b)–2(d). The transmittance and reflectance were measured with a commercially available PerkinElmer 900 spectrometer. The nanodiscs feature a plasmonic resonance at the wavelength $\lambda = 0.95\,\mu$m corresponding to a minimum in the transmittance and a maximum in the reflectance. The phase of the transmission coefficient undergoes a phase jump close to π at the wavelengths around $\lambda = 0.95\,\mu$m, where the amplitude of the transmission coefficient has a minimum. The phase jumps at about $0.65\,\mu$m in the reflection phase (Fig. 2(d)) are caused by the increasing noise level due to low sensitivity of optical spectrum analyzer in this region. Additionally, phase jumps at the borders of the measured spectral range can arise as numerical artefacts due to the Fourier transform of a finite function. The comparison of the measured and simulated spectra shows that the position of the plasmonic resonance is shifted in the simulations by about $\Delta\lambda = 20\,$nm relative to the measurements. The difference in the resonance half width was estimated to be about 40 nm.

One can see that these slight deviations in the resonance position and the resonance width between the measured and simulated spectra result in a difference of the phases, which reach values up to $\Delta\phi = 0.5$ rad at the wavelength around $\lambda = 1\,\mu$m. As a result, already minor differences between simulated and measured spectra lead to a notable error in the assessment of correct phase information which cannot be tolerated in the design of potential optical elements.

The second example at which we demonstrate the power of the introduced technique is a fishnet metasurface designed to realize symmetric and antisymmetric resonances at $\lambda = 0.8\,\mu$m and $\lambda = 1.4\,\mu$m, respectively. A scanning electron microscope image of the fabricated structure and the geometry parameters can be found in Fig. 3(a) and the caption. In Figs. 3(b)–3(d), the measured and simulated spectra and phases are presented for the polarization state of the incidence light shown in Fig. 3(a). Under these illumination conditions, the symmetric and antisymmetric resonances at the wavelengths around $\lambda = 0.8\,\mu$m and $\lambda = 1.4\,\mu$m can be excited. At the wavelengths of the antisymmetric resonance, a dip in the phase of the transmission appears that evidences a negative phase velocity of light. At the wavelengths around $1.1\,\mu$m, where the effective impedance of the metasurface approaches unity, the reflectance passes the zero point and the phase of the reflection undergoes a phase jump close to π.

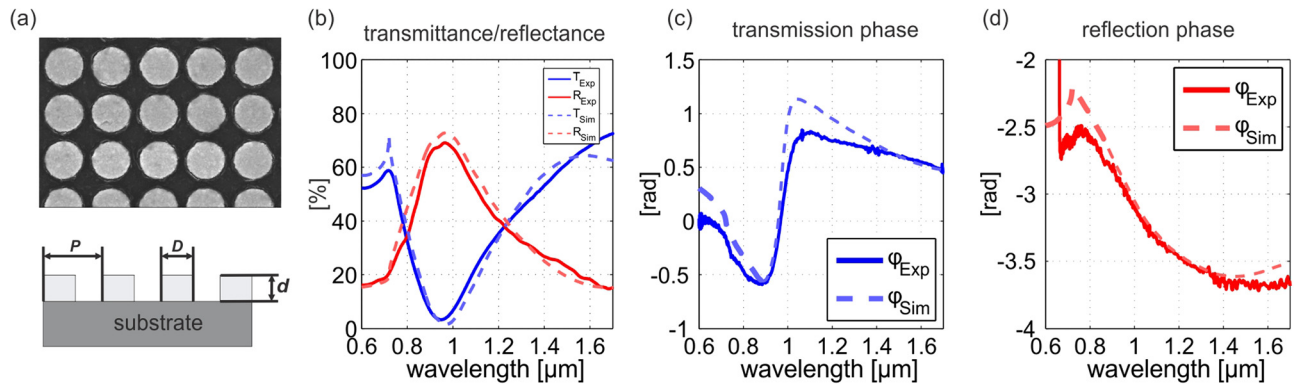

FIG. 2. (a) Electron microscopy image of a metasurface composed of nanodiscs with the following geometrical parameters: $P = 500\,$nm, $D = 350\,$nm, $d = 30\,$nm. (b)–(d) The measured and simulated transmittance and reflectance, the phase of transmission and the phase of reflection coefficients, respectively. The measured and simulated curves are labeled with "Exp" and "Sim," respectively.

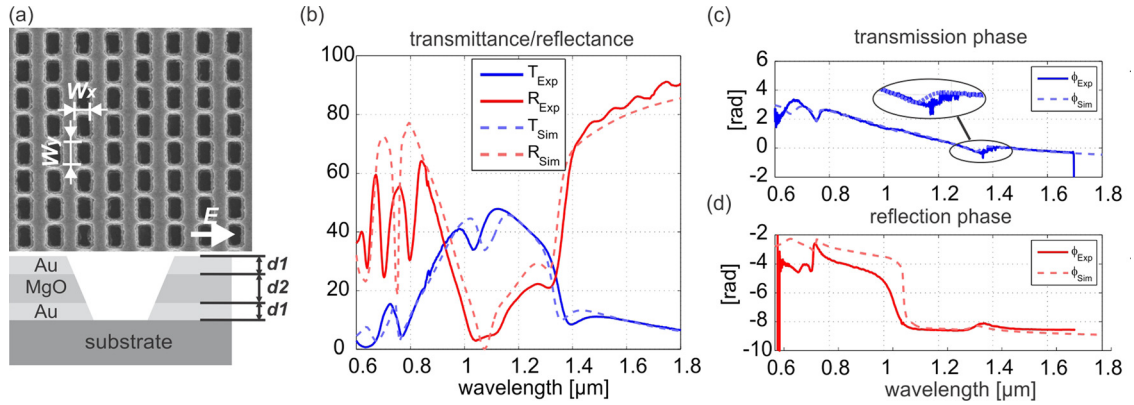

FIG. 3. (a) Electron microscopy image of a metasurface with a fishnet topology whose geometrical parameters are: $P_x = P_y = 500\,\text{nm}$, $W_x = 180\,\text{nm}$, $W_y = 380\,\text{nm}$, $d_1 = 20\,\text{nm}$, $d_2 = 40\,\text{nm}$. (b)–(d) The measured and simulated transmittance and reflectance, the phase of transmission and the phase of reflection coefficients, respectively. The measured and simulated curves are labeled with "Exp" and "Sim," respectively.

Obviously, due to the more complex geometry of the fishnet, the reconstruction of the real geometry of the structure in the numerical model is hard to achieve. In Fig. 4, the difference between measured and simulated data is shown for transmittance $|\Delta T| = |T_{Exp} - T_{Sim}|$, reflectance $|\Delta R| = |R_{Exp} - R_{Sim}|$, transmission phase $|\Delta\phi_t| = |\phi_{t,Exp} - \phi_{t,Sim}|$, and reflection phase $|\Delta\phi_r| = |\phi_{r,Exp} - \phi_{r,Sim}|$. In this case, the deviations of the position of the resonances and the amplitudes results in the transmission phase deviate up to 0.4 rad between measurements in simulations in the spectral position of the antisymmetric resonance and reflection phase deviation up to 4 rad in the spectral position of the symmetric resonance. As in the first example, such errors are certainly not to be tolerated when it comes to the performance optimization of nanostructured metasurfaces acting as steering and guiding elements for light on the nanoscale.[1–5]

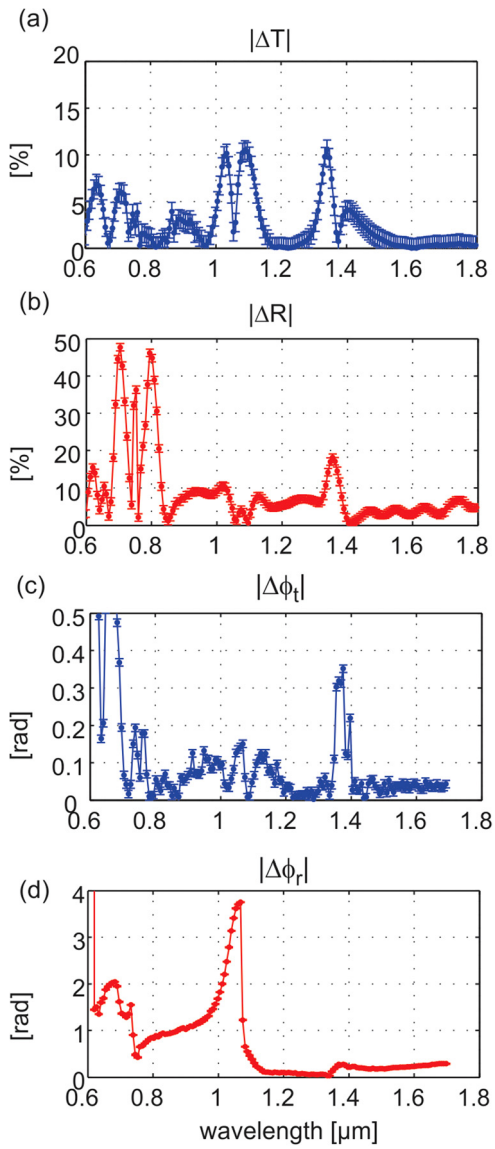

FIG. 4. Difference between the measured and simulated (a) transmittance, (b) reflectance, (c) transmission phase, (d) reflection phase for the fishnet metasurface as shown in Fig. 3(a). The error bars show the measurements accuracy.

To conclude, we have shown on the basis of a universal Kramers-Kronig transformation analysis that the use of the widely applied indirect methods is inadequate for the accurate performance assessment and characterization of complex metasurfaces. To solve this long-standing issue and to allow for an efficient feedback-loop between design and practical implementation of nanostructured metasurfaces, we have introduced an original experimental technique. Our direct method allows for determination of the phase delay accumulated by visible and near-infrared light in transmissive and reflective interaction with nanostructured metasurfaces in an ultrabroad spectral range with an unprecedented accuracy (± 0.02 rad). In terms of reliability and accuracy, this performance benchmark was shown to be superior to common numerical modeling of complex nanostructures and is applicable for a wide range of almost arbitrary optical media. Further extensions of our method, e.g., to address polarization-rotating metasurfaces or oblique incidence amplitude and phase measurements, can be implemented straightforward.

This work has been supported by the German Federal Ministry of Education and Research (PhoNa and MetaMat) and the Thuringian State Government (MeMa).

[1]A. V. Kildishev, A. Boltasseva, and V. M. Shalaev, Science **339**, 1232009 (2013).
[2]N. Yu, P. Genevet, M. A. Kats, F. Aieta, J.-P. Tetienne, F. Capasso, and Z. Gaburro, Science **334**, 333–337 (2011).
[3]F. Aieta, P. Genevet, N. Yu, M. A. Kats, Z. Gaburro, and F. Capasso, Nano Lett. **12**, 1702–1706 (2012).

[4]B. Walther, C. Helgert, C. Rockstuhl, F. Setzpfandt, F. Eilenberger, E.-B. Kley, F. Lederer, A. Tünnermann, and T. Pertsch, Adv. Mater. **24**, 6251 (2012).
[5]S. Larouche, Y.-J. Tsai, T. Tyler, N. M. Jokerst, and D. R. Smith, Nature Mater. **11**, 450–454 (2012).
[6]V. Drachev, W. Cai, U. Chettiar, H. Yuan, A. Sarychev, A. Kildishev, G. Klimeck, and V. Shalaev, Laser Phys. Lett. **3**, 49–55 (2006).
[7]G. Dolling, C. Enkrich, M. Wegener, C. M. Soukoulis, and S. Linden, Science **312**, 892–894 (2006).
[8]S. Zhang, W. Fan, N. C. Panoiu, K. J. Malloy, R. M. Osgood, and S. R. J. Brueck, Phys. Rev. Lett. **95**, 137404 (2005).
[9]B. Kanté, J.-M. Lourtioz, and A. de Lustrac, Phys. Rev. B **80**, 205120 (2009).
[10]X. Zhang, M. Davanço, K. Maller, T. W. Jarvis, C. Wu, C. Fietz, D. Korobkin, X. Li, G. Shvets, and S. R. Forrest, Opt. Express **18**, 17788–17795 (2010).
[11]M. G. Nielsen, A. Pors, O. Albrektsen, M. Willatzen, and S. I. Bozhevolnyi, J. Opt. **13**, 055106 (2011).
[12]K. O'Brien, N. D. Lanzillotti-Kimura, H. Suchowski, B. Kante, Y. Park, X. Yin, and X. Zhang, Opt. Lett. **37**, 4089–4091 (2012).
[13]R. H. Young, J. Opt. Soc. Am. **67**, 520–522 (1977).
[14]W. S. K. Kozima and P. N. Schatz, J. Opt. Soc. Am. **56**, 181–184 (1966).
[15]W. N. Hansen, J. Opt. Soc. Am. **63**, 793–802 (1973).
[16]B. Gallinet, A. M. Kern, and O. J. F. Martin, J. Opt. Soc. Am. A **27**, 2261–2271 (2010).
[17]L. Lepetit, G. Chériaux, and M. Joffre, J. Opt. Soc. Am. B **12**, 2467–2474 (1995).
[18]E. Pshenay-Severin, F. Setzpfandt, C. Helgert, U. Hübner, C. Menzel, A. Chipouline, C. Rockstuhl, A. Tünnermann, F. Lederer, and T. Pertsch, J. Opt. Soc. Am. B **27**, 660–666 (2010).
[19]See supplementary material at http://dx.doi.org/10.1063/1.4881332 for details concerning the setup and numerical calculations.
[20]A. Pashkin, M. Kempa, H. Nemec, F. Kadlec, and P. Kuzel, Rev. Sci. Instrum. **74**, 4711–4717 (2003).
[21]M. G. Moharam, E. B. Grann, D. A. Pommet, and T. K. Gaylord, J. Opt. Soc. Am. A **12**, 1068–1076 (1995).